Article

Discovery Medicine 2025; 37(194): 515–524
https://doi.org/10.24976/Discov.Med.202537194.43

ACSL6-Mediated Cell Ferroptosis by Inhibiting AMPK Pathway in Periodontitis Stem Cells

YaTing Chang[1,2,†], LongHang Chou[1,2,†], ChongMai Zeng[1,2], PeiRu Li[1,2], Orkideh Shafiee Allaf[1,2], YuKun Lu[1,2], Yue Xu[1,2,*]

[1]Department of Orthodontics, Hospital of Stomatology, Guanghua School of Stomatology, Sun Yat-sen University, 510055 Guangzhou, Guangdong, China
[2]Guangdong Provincial Key Laboratory of Stomatology, 510055 Guangzhou, Guangdong, China
*Correspondence: kou9315@hotmail.com (Yue Xu)
[†]These authors contributed equally.
Published: 20 March 2025

Background: Periodontitis is an immunoinflammatory disease. Ferroptosis is a type of inflammation-associated cell death. The article aims to investigate the expression, role, and mechanism of the ferroptosis-related gene acyl-CoA synthetase long-chain family member 6 (*ACSL6*) in periodontitis

Methods: Ferroptosis-related genes were identified using the Gene Expression Omnibus dataset and the Kyoto Encyclopedia of Genes and Genomes pathway. *ACSL6* expression was validated using quantitative reverse-transcription polymerase chain reaction in patients with periodontitis. Human periodontal ligament fibroblasts (hPDLFs) were isolated and characterized. Following treatment, related experiments were performed to evaluate iron levels, reactive oxygen species (ROS) production, cell viability, *ACSL6* expression, and ferroptosis-related proteins in hPDLFs.

Results: In this study, 185 genes were upregulated, and 102 were downregulated in the periodontitis group ($p < 0.05$). *ACSL6*, a ferroptosis-related gene, exhibited high expression levels in periodontitis tissues ($p < 0.05$). *Porphyromonas gingivalis* lipopolysaccharide (*P. gingivalis*-LPS) upregulated *ACSL6* ($p < 0.05$), downregulated ferroptosis-related genes (glutathione peroxidase 4 ($p < 0.001$) and cystine/glutamate transporter (Solute Carrier Family 7 Member 11) ($p < 0.01$)) and phosphor (p)-AMP-activated protein kinase (AMPK) ($p < 0.05$), reduced cell viability ($p < 0.001$), and elevated iron ($p < 0.001$) and ROS levels ($p < 0.001$) in hPDLFs. *ACSL6* silencing could counteract the effects of *P. gingivalis*-LPS ($p < 0.01$). Furthermore, AMPK inhibitors lessen the effect of *ACSL6* silencing ($p < 0.01$).

Conclusions: The ferroptosis-related gene *ACSL6* was highly expressed in periodontitis tissues, and *ACSL6* silencing enhanced viability and inhibited ferroptosis in *P. gingivalis*-LPS-mediated hPDLFs by upregulating the AMPK pathway.

Keywords: *ACSL6*; ferroptosis; periodontitis; human periodontal ligament fibroblasts; AMPK pathway

Introduction

Periodontitis is a common infectious disease in humans, which is characterized by periodontal tissue inflammation, alveolar bone destruction, and tooth loss [1]. Dysbiosis of the oral microflora, resulting in excessive infiltration of immune cells in the periodontal tissue, is the primary cause of periodontitis [2]. Various factors, including genetics, metabolism, immunity, and inflammation, influence the progression of periodontitis. Periodontitis is associated with systemic diseases, such as cancer, obesity, and diabetes [3]. Periodontitis affects 20%–50% of the global population [4]. A recent study on the pathology of periodontitis enabled the development of novel therapies and the local application of advanced drug delivery systems [5]. However, further investigations of the molecular mechanisms in periodontitis are required to develop targeted treatments.

Cell survival or death is a crucial aspect of the inflammatory response [6]. Cellular stress induced by abnormal metabolic and biochemical processes might trigger a widespread nonapoptotic cell death, frequently called ferroptosis [7]. Ferroptosis is mainly characterized by lipid peroxides and membrane ferritin accumulation [8]. Convincing evidence revealed that ferroptosis is crucial in inflammation. The inhibition of ferroptosis has anti-inflammatory effects in some diseases [9]. Periodontitis-induced increase in butyrate levels destroys iron homeostasis by activating nuclear receptor coactivator 4-mediated ferritinophagy, resulting in the ferroptosis of human periodontal ligament fibroblasts (hPDLFs) [10]. Therefore, ferroptosis occurs in periodontitis. However, the mechanisms regulating it remain unclear.

The development of high-throughput methods in biological research has produced substantial omics data. Tran-

scriptomics facilitated by microarray analyses has enhanced our understanding of the alterations in gene expression involved in multifactorial diseases [11], including periodontitis [12–14]. We analyzed differentially expressed genes (DEGs) between patients with periodontitis and healthy individuals using the Gene Expression Omnibus (GEO) dataset GSE106090. We compared them with the Kyoto Encyclopedia of Genes and Genomes (KEGG) ferroptosis pathway genes. We found higher acyl-CoA synthetase long-chain family member 6 (*ACSL6*) expression in patients with periodontitis. However, whether *ACSL6* is involved in periodontitis progression and its potential mechanism in ferroptosis remain to be elucidated. Thus, this study further explored the mechanism of action of the ferroptosis-related gene *ACSL6* in periodontitis using *in vitro* experiments. Our findings may provide valuable insights into new strategies for treating periodontitis.

Materials & Methods

Microarray Analysis

In this study, the GEO dataset GSE106090 in the periodontal tissues of patients with periodontitis (n = 6) and healthy individuals (n = 6) was examined. Original data were analyzed using the R package GEOquery (version 3.19, Bioconductor, Bethesda, MD, USA), and DEGs were screened using the R package limma. The screening criteria for constructing heat maps and scatter plots were log fold change (logFC) $\geq$1.5 and $p \leq 0.05$. Subsequently, the data were combined with those from the KEGG ferroptosis pathway genes for differential analysis, and a heat map was generated. To investigate the role of *ACSL6* in periodontitis, the GEO dataset was used to analyze *ACSL6* expression in periodontitis tissues.

Tissue Sample

Tissues were collected from 20 donors. The inclusion criteria for the healthy group (10) were as follows: healthy human first premolars extracted for orthodontic reasons and age of 10–14 years. The inclusion criteria for the periodontitis group (10) were as follows: partially or fully dentate patients and age of 10–14 years. The exclusion criteria were as follows: smoking, presence of any systemic disease such as type 1 and 2 diabetes, or allergy; and use of drugs including immunosuppressive agents, corticosteroids, and antibiotics within 1 month before the surgery. Donors and their family members consented to this institutionally approved study protocol.

Isolation of hPDLFs

Primary hPDLFs were collected from orthodontic extractions of healthy premolars. Primary hPDLFs were isolated using an enzyme digestion method, as reported previously [15,16]. Briefly, fresh teeth were placed in Hank's (A318-02, HyClone, South Logan, UT, USA) supplemented with 1% double antibodies (penicillin and streptomycin, P1400, Solarbio, Beijing, China). The periodontal ligament tissues were scraped from the middle third of the root surface with a blade and scalpel under sterile conditions and placed in phosphate-buffered saline (PBS) (P1010, Solarbio) supplemented with 1% double antibodies. Then, the tissues were seeded onto culture flasks after digestion with 0.1% type I collagenase (SCR103, Sigma, St. Louis, MO, USA) for 30 min at 37 °C. hPDLFs were collected after centrifugation (500 $\times$g, 5 min). hPDLFs were cultured in Dulbecco's modified eagle medium (DMEM) (11965, Solarbio) with 10% fetal bovine serum and 1% double antibodies. Cells from the third to sixth passages were applied in the experiments. The hPDLFs were negative for mycoplasma. Cytomorphological characterization was conducted using an immunofluorescence (IF) assay.

IF Assay

hPDLFs were inoculated on coverslips in six-well plates. After 24 h of incubation, the cell density was 60%–70%. Cells were fixed and permeabilized using paraformaldehyde and 0.2% Triton-X-100. After washing, cells were blocked with 5% bovine serum albumin at 37 °C for 30 min and added with the primary antibody CD44 (1:100; 15675-1-AP, Proteintech, Wuhan, China) and vimentin (1:100; 22031-1-AP, Proteintech) overnight in a wet box at 4 °C and the secondary antibody (SA00013-2; 1:1000; Proteintech) in a dark chamber for 2 h. Cells were processed with a 4′,6-diamidino-2-phenylindole (DAPI) solution (D9542, Sigma) for 30 min and sealed with an antifluorescence quencher (S2100, Solarbio). Protein expression and localization were captured using a fluorescence microscope (EVOS M5000, Evosfl Auto, Life Technologies, Gaithersburg, MD, USA).

Flow Cytometry

hPDLFs were obtained and inoculated in six-well plates. After 24 h of incubation, the cell density was 80%. After washing, cells (1×10^6) were incubated with an antibody at 25 °C for 30 min without light. The expressions of CD29, CD44, CD31, and CD14 were detected using BD FACSCanto II (BD Biosciences, San Jose, CA, USA). Antibody information was as follows: Allophycocyanin (APC)-CD44 (ab81424, Abcam, Cambridge, MA, USA), APC-CD29 (BD-559883, BD Biosciences), Brilliant Violet 421-CD31 (303123, Biolegend, San Diego, CA, USA), Brilliant Violet 421-CD14 (565283, BD Biosciences), Brilliant Violet 421 mouse IgG1 (562438, BD Biosciences), and APC mouse Immunoglobulin G (IgG) 1 (550854, BD Biosciences).

Cell Treatment

Initially, to identify the optimal treatment concentration, hPDLFs were processed with *Porphyromonas gingivalis* lipopolysaccharide (*P. gingivalis*-LPS; 0, 1,

3, or 10 mg/L). Subsequently, hPDLFs were transfected with small interfering RNAs (siRNAs) targeting *ACSL6* (three different siRNAs) or a negative control (NC) using Lipofectamine™ 2000 (BL623B, BioSharp, Hefei, China). The siRNA sequences were as follows: si-*ACSL6*-1 (F: 5′-AUAGUAGUGGGUAAGUAGCUG-3′, R: 5′-GCUACUUACCCACUACUAUGA-3′), si-*ACSL6*-2 (F: 5′-UAUCAUUCCUGAUGAUUCCAC-3′, R: 5′-GGAAUCAUCAGGAAUGAUAGU-3′), si-*ACSL6*-3 (F: 5′-ACCAAAAAGGCCUUUAAGCUG-3′, R: 5′-GCUUAAAGGCCUUUUUGGUAG-3′), and NC (5′-UCACCCAGAUGCCGCUAU-3′) (GenePharma, Shanghai, China). Because *si-ACSL6*-3 offered the best knockdown, it was selected for the subsequent experiments. The hPDLFs were grouped according to treatment as control (unprocessed hPDLFs), LPS (10 mg/L *P. gingivalis*-LPS-processed hPDLFs), and LPS + *si-ACSL6*-3 (hPDLFs transfected with *si-ACSL6*-3 and processed with *P. gingivalis*-LPS). To confirm the role of ferroptosis, the hPDLFs were grouped into control (unprocessed hPDLFs), LPS (*P. gingivalis*-LPS-processed hPDLFs), and LPS + Fer-1 (Fer-1 preprocessed the cells for 30 min and added LPS processed for 24, 48, and 72 h). To validate whether *ACSL6* mediated the ferroptosis through the AMP-activated protein kinase (AMPK) pathway, hPDLFs were divided into NC (hPDLFs transfected with NC and then processed with PBS for 48 h), NC + LPS (hPDLFs transfected with NC and then processed using *P. gingivalis*-LPS for 48 h), *si-ACSL6* (hPDLFs transfected with *si-ACSL6* and processed using PBS for 48 h), *si-ACSL6* + Dorsomorphin (Dor, CM00836, Proteintech) (hPDLFs transfected with *si-ACSL6* and preprocessed using Dor for 24 h followed by *P. gingivalis*-LPS treatment for 48 h).

Quantitative Reverse-Transcription Polymerase Chain Reaction (qRT-PCR)

Total RNA was extracted with Trizol (15596026, Invitrogen, Gaithersburg, MD, USA) and transcribed into complementary DNA with a reverse-transcription kit (#CW2569, Beijing ComWin Biotech, Beijing, China). SYBR Green qPCR Mix (Invitrogen) was adopted to determine the relative expression of *ACSL6* on the ABI 7900 system (4351405, ABI, CA, USA) using qRT-PCR. Gene levels were calculated by the $2^{-\Delta\Delta Ct}$ method. The primer sequences were *ACSL6*-F: 5′-GACCTTCTTCCTCGTGTCGG-3′, *ACSL6*-R: 5′-AACCAGTAGGCAAGGATGGC-3′, glyceraldehyde-3-phosphate dehydrogenase (*GAPDH*)-F: 5′-AGAAGGCTGGGGCTCATTTG-3′, and *GAPDH*-R: 5′-AGGGGCCATCCACAGTCTTC-3′.

Western Blotting

Total proteins were extracted from hPDLFs using radioimmunoprecipitation assay lysis buffer (P0013B, Beyotime Biotechnology, Shanghai, China). After protein quantification using a bicinchoninic acid (BCA) kit (BL521A, Biosharp, Hefei, China), the protein extracts were mixed with sodium dodecyl-sulfate polyacrylamide gel electrophoresis. The proteins were electrotransferred onto polyvinylidene difluoride membranes and blocked with 5% skim milk solution for 2 h, processed with primary antibodies against ACSL6 (1:2000; A7965, ABclonal Technology, Wuhan, China), glutathione peroxidase 4 (GPX4, 1:2000; A11243, ABclonal Technology), cystine/glutamate transporter (Solute Carrier Family 7 Member 11 (SLC7A11), 1:2000; A13685, ABclonal Technology), Phospho-AMPKα1-S496 (1:2000; AP1002, ABclonal Technology), and GAPDH (1:2000; A19056, ABclonal Technology) overnight at 4 °C, and horseradish peroxidase (HRP)-conjugated goat anti-rabbit IgG (H + L) (1:5000; AS014, ABclonal Technology). Signals were displayed using enhanced chemiluminescence. The band's gray value was analyzed using ImageJ 1.8 (National Institutes of Health, Bethesda, MD, USA) and normalized to GAPDH or AMPKα (1:5000; 10929-2-AP, proteintech) (for p-AMPK).

Cell Counting Kit-8 (CCK-8)

The cells were digested using trypsin, resuspended in PBS, and seeded into 96-well plates (100 µL, 5×10^3 cells/well). After incubation, the hPDLFs were added with 10 µL of CCK-8. Cell proliferation was determined after 24, 48, and 72 h using a bio-Tek microplate analyzer (MB-530, Heales, Jinan, China) at 450 nm.

Iron Detection

Iron was identified using the Intracellular Iron Colorimetric Assay Kit (E1042, ApplyGen, Beijing, China). Briefly, cells cultured in iron-containing DMEM were washed with 2 mL of precooled PBS. The cells were lysed by incubating them with 200 µL/well lysis buffer for 2 h. Thereafter, the standard was diluted by mixing the buffer and 4.5% solution at a ratio of 1:1. The samples were transferred to 1.5-mL centrifuge tubes, and blank control, standard, and sample tubes were used. All tubes were processed at 60 °C for 1 h. An iron ion reagent (30 µL) was introduced into each tube and mixed well. After 30 min of incubation, 200 µL of the samples were transferred to a 96-well plate, the absorbance was monitored at 550 nm, and the iron concentration was determined.

Reactive Oxygen Species (ROS) Detection

ROS produced by hPDLFs were detected using a ROS assay kit (S0033S, Beyotime Biotechnology). Briefly, cells (1×10^6) were centrifuged and washed. The cell pellets were resuspended in diluted dichlorodihydrofluorescein diacetate (1:1000) for 20 min and mixed every 5 min. After washing, the cells were observed under a fluorescence microscope [17].

Statistical Analysis

Data were represented as means ± standard deviations. The analysis was performed using GraphPad Prism 8.0 (GraphPad Software, Inc., La Jolla, CA, USA) (Student's *t*-test or one-way analysis of variance (Tukey's post-hoc test)). $p < 0.05$ denoted significance.

Results

Expression Analysis of Ferroptosis-Related Genes in Periodontitis

Initially, the GEO dataset GSE106090 was analyzed. Fig. 1A depicts a heat map of the DEGs in the periodontal tissues of the periodontitis and healthy groups. A scatter plot analysis of the DEGs was performed. In the periodontal tissue of the periodontitis group, 185 genes were upregulated, and 102 were downregulated (Fig. 1B). Using the KEGG pathway analysis, the DEGs related to ferroptosis were identified. The heat map showed the ferroptosis-related genes with relatively high differential expression; *ACSL*6, a ferroptosis-related gene, is highly expressed in the periodontitis group relative to the healthy group (Fig. 1C).

P. gingivalis-LPS Enhanced ACSL6 Expression and Ferroptosis and Weakened Cell Viability by Ferroptosis in hPDLFs

Based on the GEO data, *ACSL6* levels were higher in the periodontitis group than in the healthy group (Fig. 2A, $p < 0.001$) and the qRT-PCR data demonstrated that *ACSL6* was highly expressed in the periodontitis group ($p = 0.0131$; Fig. 2B). To further analyze the role and mechanism of *ACSL6* in periodontitis, hPDLFs were initially extracted using an enzyme digestion method [15,16]. IF data demonstrated that periodontal stem cell marker proteins CD44 and vimentin were positive in isolated cells (**Supplementary Fig. 1A**). Flow cytometry also showed that CD29 and CD44 were positive but CD31 and CD14 were negative in isolated cells (**Supplementary Fig. 1B**). These results indicate that we have successfully isolated hPDLFs.

Then, hPDLFs were processed with *P. gingivalis*-LPS (0, 1, 3, or 10 mg/L), and *ACSL6* expression was determined using qRT-PCR. As shown in Fig. 2C, relative to unprocessed cells, *ACSL6* expression increased in *P. gingivalis*-LPS-processed cells ($p < 0.05$). Western blotting revealed that relative to the hPDLF cells, the ACSL6 level increased ($p < 0.001$), and the protein levels of ferroptosis suppressors GPX4 and SLC7A11 were reduced ($p < 0.01$) in *P. gingivalis*-LPS-processed hPDLF cells (Fig. 2D,E). Thus, *P. gingivalis*-LPS was employed in the follow-up experiments. Moreover, ROS and iron levels were increased after 10-mg/L *P. gingivalis*-LPS treatment in hPDLF cells ($p < 0.001$; Fig. 2F,G). Furthermore, *P. gingivalis*-LPS reduced the cell viability of hPDLFs, and the ferroptosis inhibitor Fer-1 attenuated this phenomenon ($p < 0.001$; Fig. 2H). These findings indicate that *P. gingivalis*-LPS induces *ACSL6* expression and promotes ferroptosis in hPDLFs.

ACSL6 Silencing Promoted Viability and Reduced Ferroptosis in hPDLFs Induced by P. gingivalis-LPS

ACSL6 was silenced in hPDLFs by transfection with *ACSL6* siRNAs (si-*ACSL6*). The transfection of si-*ACSL6*-1, si-*ACSL6*-2, and si-*ACSL6*-3 efficiently decreased the expression level of *ACSL6* relative to the NC group, particularly si-*ACSL6*-3 ($p < 0.001$; Fig. 3A). Western blotting results further confirmed the successful knockdown of *ACSL6* by transfection ($p < 0.05$; Fig. 3B). Thus, si-*ACSL6*-3 was used in the follow-up experiments. CCK-8 showed reduced proliferation of *P. gingivalis*-LPS-processed hPDLFs relative to that in the control group on day 3, and *ACSL6* silencing prevented this decrease ($p < 0.01$; Fig. 3C). Iron levels were increased after *P. gingivalis*-LPS therapy ($p < 0.001$), and *ACSL6* silencing reversed this abnormal increase in cellular iron ions ($p < 0.001$; Fig. 3D). Furthermore, Western blot analyses showed that GPX4 and SLC7A11 expression levels reduced after treating hPDLFs with *P. gingivalis*-LPS ($p < 0.01$). The decrease in GPX4 and SLC7A11 levels mediated by *P. gingivalis*-LPS was reversed by *ACSL6* interference ($p < 0.05$; Fig. 3E,F). Finally, ROS production was monitored. As depicted in Fig. 3G, the ROS levels in the *P. gingivalis*-LPS group were increased relative to that in the control group, which was reversed by *ACSL6* silencing ($p < 0.001$). Thus, *ACSL6* could affect *P. gingivalis*-LPS-induced cell ferroptosis.

ACSL6 Silencing Attenuated Cell Ferroptosis by Inhibiting the AMPK Pathway in P. gingivalis-LPS-Mediated hPDLFs

A previous study indicated that *ACSL6* inhibited the AMPK pathway [18]. The AMPK pathway was also inhibited ferroptosis [19,20]. Our results also showed that *P. gingivalis*-LPS promoted *ACSL6* expression. Thus, *ACSL6* may have mediated the AMPK pathway. Western blotting demonstrated that *ACSL6* silencing upregulated p-AMPK in hPDLFs ($p < 0.001$; Fig. 4A). Meanwhile, relative to the NC group, p-AMPK, SLC7A11, and GPX4 expressions were decreased in hPDLFs treated with *P. gingivalis*-LPS. *ACSL6* silencing increased these protein levels, which were reversed by the AMPK inhibitor Dor in *P. gingivalis*-LPS-processed hPDLFs ($p < 0.05$; Fig. 4B,C). The cell viability and ROS levels revealed the same trend with the p-AMPK expression ($p < 0.001$; Fig. 4D,E). These findings indicated that *ACSL6*-mediated cell ferroptosis mediated by *P. gingivalis*-LPS by inhibiting the AMPK pathway in hPDLFs.

Discussion

Periodontitis is an immunoinflammatory disease characterized by the progressive degradation of bone and con-

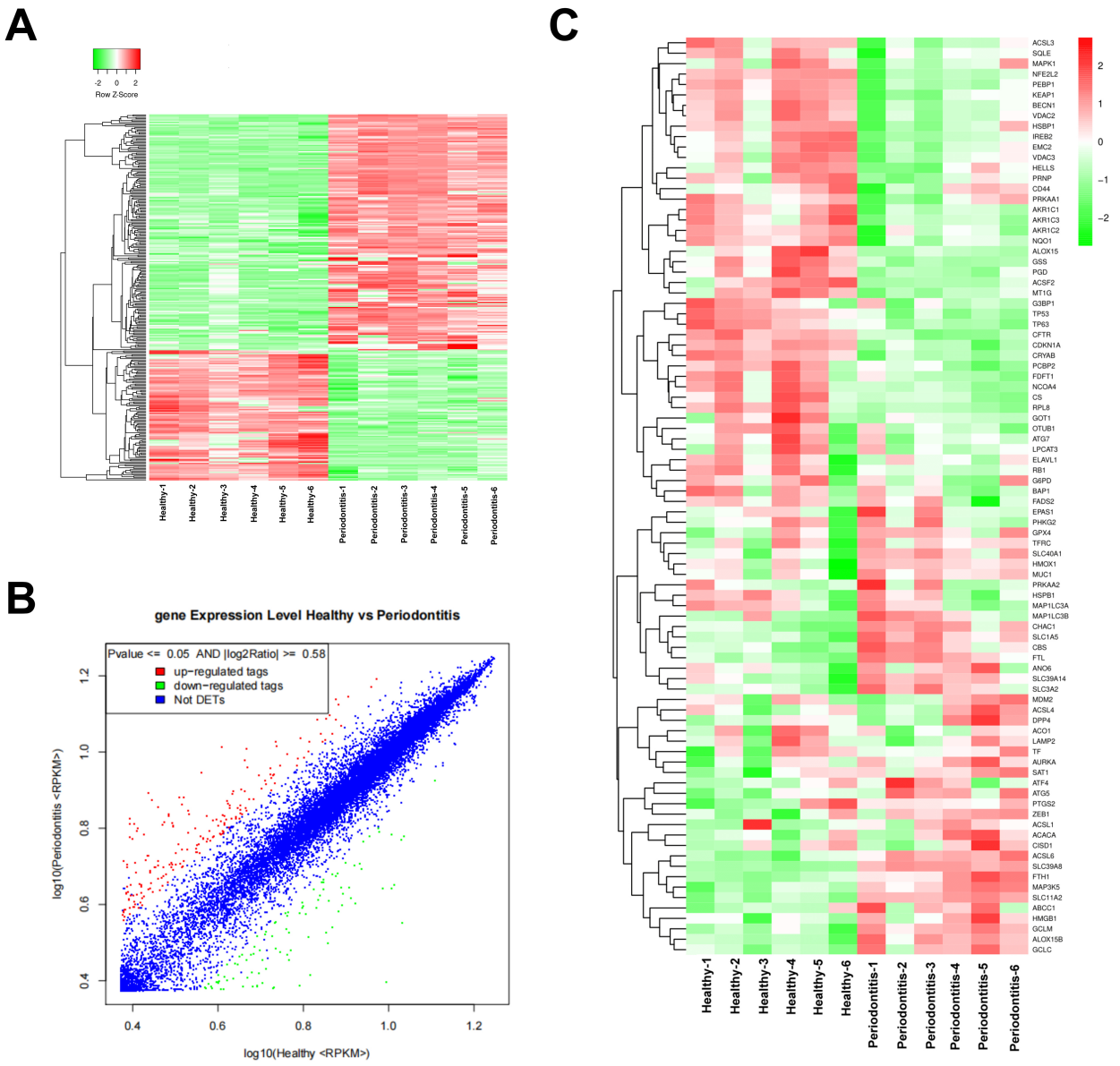

Fig. 1. Expression analysis of ferroptosis-related genes in periodontitis. (A) Heat map of differentially expressed genes between the healthy and periodontitis groups in a Gene Expression Omnibus (GEO) dataset. (B) Scatter plot of differentially expressed genes in a GEO dataset. RPKM, Reads Per Kilobase of exon model per Million mapped reads; DETs, Differential Expressed Transcripts. (C) Heat map analysis of differentially expressed genes in the Kyoto Encyclopedia of Genes and Genomes ferroptosis pathway. The full names of the genes in the heat map are in **Supplementary Table 1**.

nective tissues in the periodontal region [21]. Both periodontal bacteria and host immunity are involved in the pathological process of periodontal diseases [22,23]. The molecular mechanisms in the physiopathology of periodontitis must be elucidated to develop targeted therapies. Ferroptosis is involved in periodontitis [10]. However, the precise mechanisms underlying ferroptosis activation in periodontitis remain unclear. This study discovered a high expression of *ACSL6* in periodontitis tissues utilizing microarray analysis and investigated the involvement of *ACSL6* in periodontitis. The results revealed that the protein and gene expressions of *ACSL6* were higher in periodontitis. Moreover, *ACSL6* mediated *P. gingivalis*-LPS-induced cell ferroptosis by the AMPK pathway. To our knowledge, this is the first report considering the role and potential mechanism of *ACSL6* in periodontitis.

Microbial biofilms and host-mediated inflammation induce periodontitis. Among the bacteria involved, *P. gingivalis* critically disrupts the host's immune homeostasis. *P. gingivalis* uses LPS, proteases, fimbriae, and other virulence factors to facilitate bacterial colonization [24]. hPDLFs loss is one of the primary factors preventing periodontal tissue regeneration [25]. During the development of periodontitis, the activation of various cell death path-

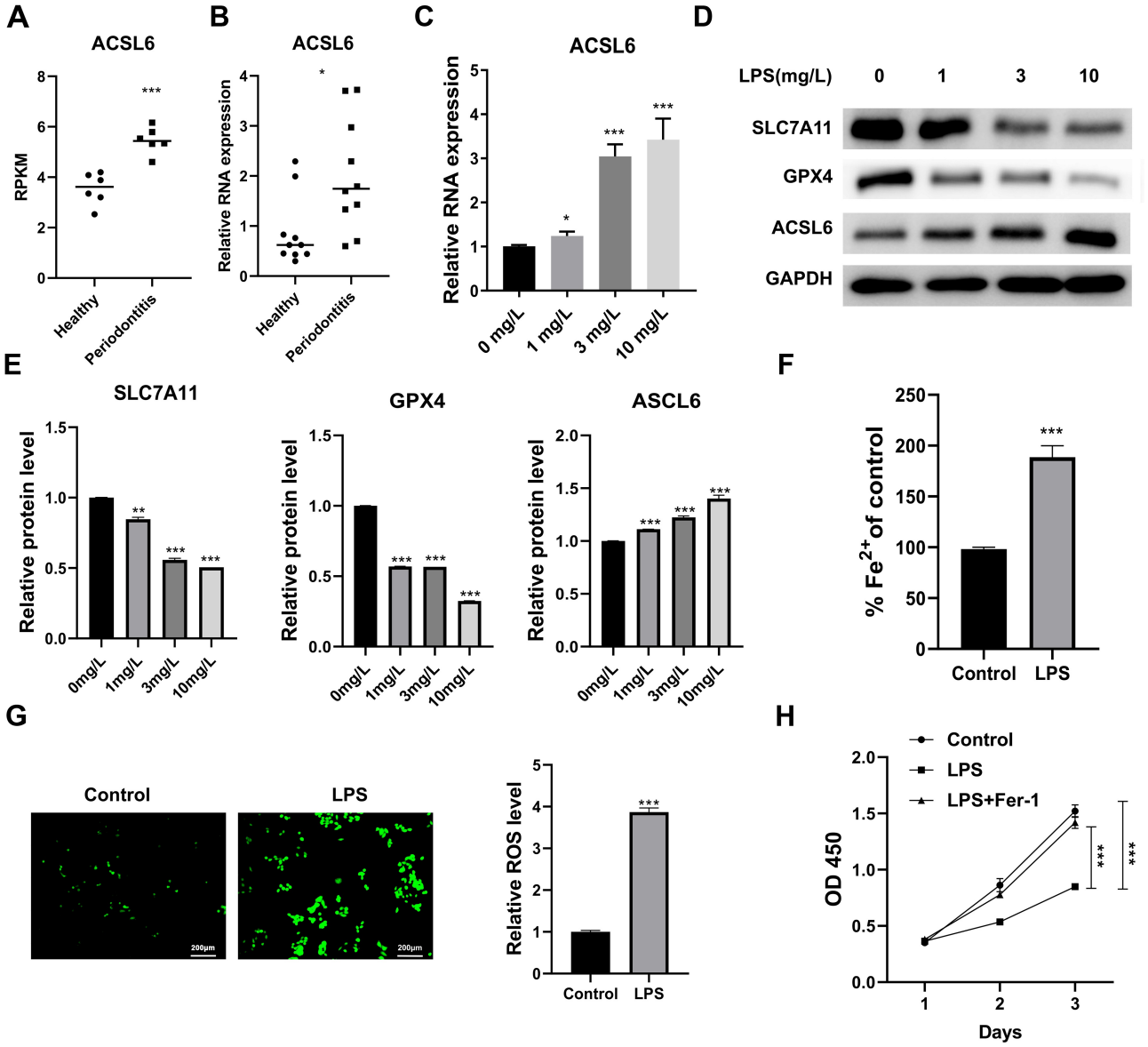

Fig. 2. ***Porphyromonas gingivalis*** **lipopolysaccharide (*P. gingivalis*-LPS) upregulated acyl-CoA synthetase long-chain family member 6 (*ACSL6*), enhanced ferroptosis, and inhibited cell viability by ferroptosis in human periodontal ligament fibroblasts (hPDLFs).** (A) Gene Expression Omnibus data (n = 6) of *ACSL6* expression in healthy and periodontitis tissues. (B) Quantitative reverse-transcription polymerase chain reaction (qRT-PCR) analysis (n = 10) of *ACSL6* expression in healthy and periodontitis tissues. (C) After treating hPDLFs with *P. gingivalis*-LPS (0, 1, 3, or 10 mg/L), *ACSL6* expression was monitored using qRT-PCR. The experiments were conducted in triplicates. (D) Western blot analysis of the protein levels of ACSL6 and the ferroptosis suppressors glutathione peroxidase 4 (GPX4) and Solute Carrier Family 7 Member 11 (SLC7A11). The experiments were conducted in triplicates. (E) Quantitative analysis of Western blotting data (ACSL6, GPX4, and SLC7A11). The experiments were conducted in triplicates. (F) Quantification of iron levels using the Intracellular Iron Colorimetric Assay Kit. The experiments were conducted in triplicates. (G) hPDLFs were processed with *P. gingivalis*-LPS (0 and 10 mg/L) for 48 h, and reactive oxygen species (ROS) levels were monitored using a ROS assay kit. Scale bar = 200 μm. The experiments were conducted in triplicates. (H) Cell viability of hPDLFs was assessed using Cell Counting Kit-8. The experiments were conducted in triplicates. *$p < 0.05$, **$p < 0.01$, ***$p < 0.001$. GAPDH, glyceraldehyde-3-phosphate dehydrogenase.

ways, including apoptosis, pyrolysis, and necrosis, was suggested [10]. Ferroptosis is involved in periodontitis; however, research on its role in periodontitis is limited. In this study, we processed hPDLFs with *P. gingivalis*-LPS to examine the mechanism of action of *ACSL6*. *ACSL6* exhibited high expression in periodontitis, whereas the expressions of the ferroptosis suppressor genes *GPX4* and *SLC7A11* were low. To the best of our knowledge, this is the first description of the upregulation of *ACSL6* in periodontitis.

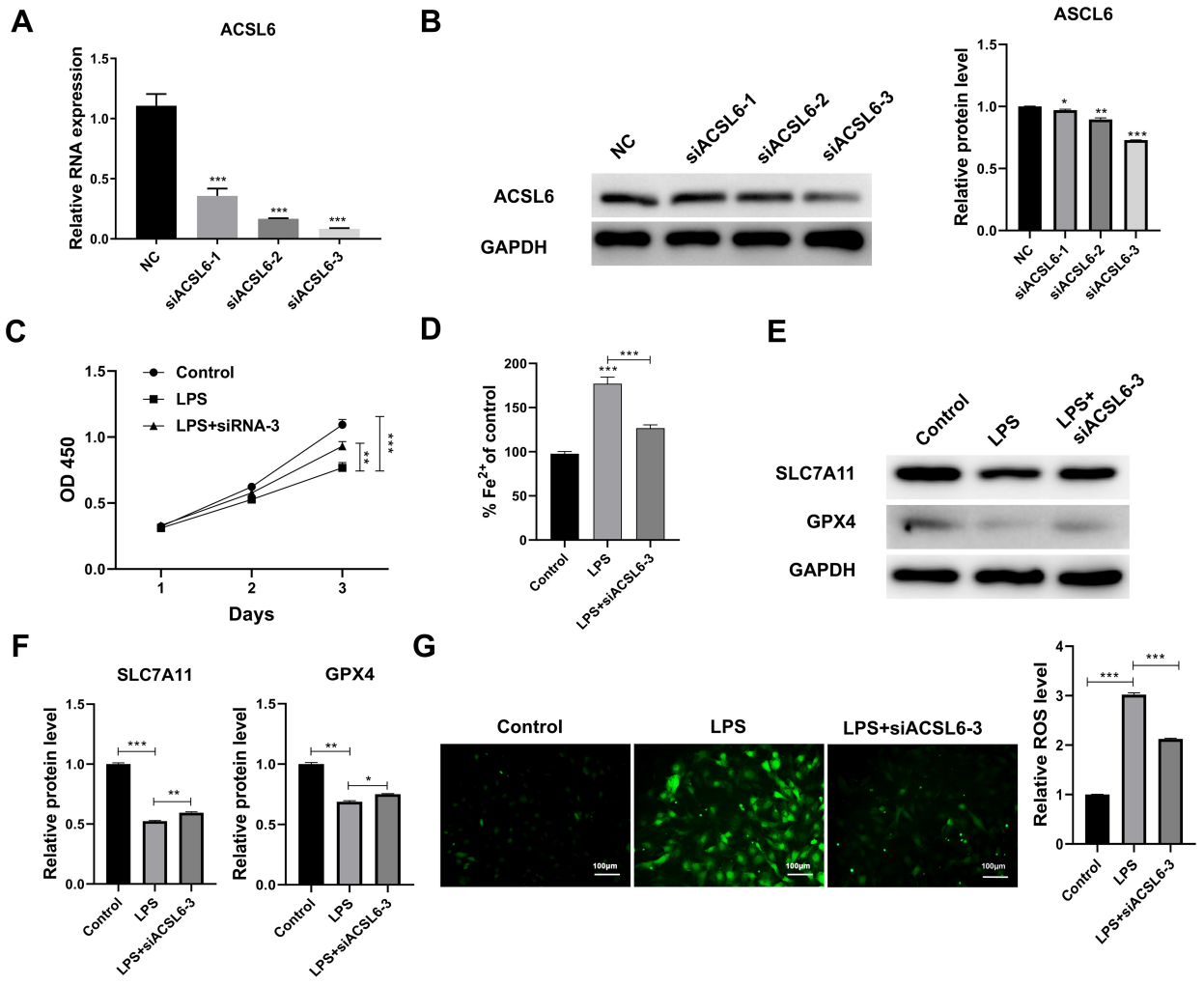

Fig. 3. Effect of *ACSL6* silencing on the viability and ferroptosis in hPDLFs induced by *P. gingivalis*-LPS. (A,B) *ACSL6* silencing efficiency in hPDLFs was monitored using quantitative reverse-transcription polymerase chain reaction and Western blotting. hPDLFs were transfected with si-*ACSL6*-3 and processed with 10 mg/L *P. gingivalis*-LPS. The experiments were conducted in triplicates. (C) Cell viability of hPDLFs was assessed using the Cell Counting Kit-8. The experiments were conducted in triplicates. (D) Quantification of iron levels using the Intracellular Iron Colorimetric Assay Kit. The experiments were conducted in triplicates. (E) Western blot analysis of ferroptosis suppressors GPX4 and SLC7A11. The experiments were conducted in triplicates. (F) Quantitative analysis of GPX4 and SLC7A11 proteins. The experiments were conducted in triplicates. (G) ROS levels were monitored using a ROS assay kit. Scale bar = 100 µm. The experiments were conducted in triplicates. * $p < 0.05$, ** $p < 0.01$, *** $p < 0.001$. NC, negative control of si-*ACSL6*.

Ferroptosis is a non-apoptotic cell death found recently and involves various physiological and pathological processes [26]. *ACSL6* is an essential factor in ferroptosis [27]. A study has indicated that *ACSL6* is a potential therapeutic target in cancer because specific inhibitors have been demonstrated to restrict the growth of cancer cells by reprograming the cellular metabolism toward fatty acid reduction [28]. Conversely, *ACSL6* may promote fatty acid synthesis, providing substrate and energy for cell proliferation [29]. *ACSL6* expression is downregulated in colorectal and various cancers [30]. A low *ACSL6* expression is associated with a poor prognosis of acute myeloid leukemia [31]. In hepatocellular carcinoma, *ACSL6* expression in cancer tissue was lower than that in adjacent tissues [32], and *ACSL6* was identified to be a protective gene in this cancer [32]. In colorectal cancer, *ACSL6* overexpression promotes fatty acid synthesis and offers intermediate metabolites and energy for cell proliferation [33]. However, the role of *ACSL6* in periodontitis is unknown. In this study, the involvement of *ACSL6* in periodontitis by silencing *ACSL6* expression was investigated. For the first time, *ACSL6* mediated *P. gingivalis*-LPS-induced cell ferroptosis.

A previous study indicated that *ACSL6* inhibited the AMPK pathway [18]. AMPK is essential in maintaining intracellular energy balance and the energy metabolism of the whole body; therefore, it can be a potential therapeu-

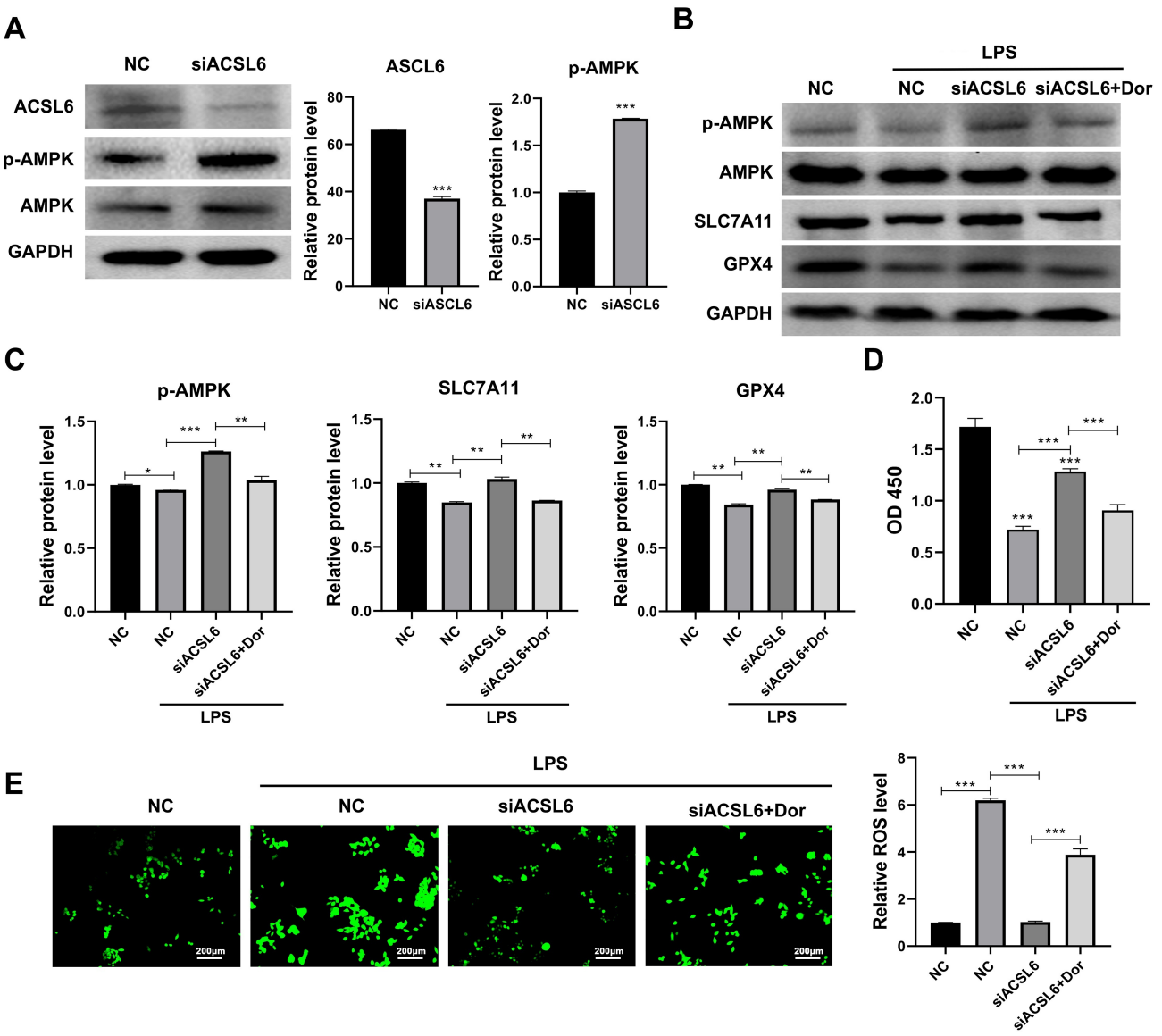

Fig. 4. *ACSL6* silencing inhibited cell ferroptosis by inhibiting the AMP-activated protein kinase (AMPK) pathway in *P. gingivalis*-LPS-mediated hPDLFs. (A)Western blot analysis of *ACSL6*, AMPK and phospho (p)-AMPK after *ACSL6* silencing. The experiments were conducted in triplicates. (B) hPDLFs were transfected with siNC or *si-ACSL6* for 24 h and processed with/without 5 μM Dorsomorphin treatment for 24 h, followed by/without 10 mg/L *P. gingivalis*-LPS treatment for 48 h. The levels of p-AMPK, GPX4, and SLC7A11 were analyzed using Western blotting. The experiments were conducted in triplicates. (C) Quantitative analysis of p-AMPK, GPX4, and SLC7A11 proteins was performed in each group. The experiments were conducted in triplicates. (D) Cell viability of hPDLFs was assessed using the Cell Counting Kit-8. The experiments were conducted in triplicates. (E) ROS levels were monitored using a ROS assay kit. Scale bar = 200 μm. The experiments were conducted in triplicates. * $p < 0.05$, ** $p < 0.01$, *** $p < 0.001$.

tic target for metabolic syndrome and cancer [34]. AMPK inhibits the nuclear factor-κB-dependent inflammatory process [35]. In *P. gingivalis*-LPS-processed Human Kidney-2 (HK-2), human umbilical vein endothelial cells, and THP-1 cells, the AMPK pathway was inhibited, and AMPK activation attenuated its effect [36,37]. Furthermore, the AMPK pathway was suppressed in ferroptosis mediated by *P. gingivalis*-LPS [19,20]. Similarly, p-AMPK expression was reduced in *P. gingivalis*-LPS-processed hPDLFs. Furthermore, this study was the first to show that the knockdown of *ACSL6*-activated p-AMPK and the AMPK pathway inhibitor Dor reversed the effect of si-*ACSL6*.

Based on the above findings, this study provided the foundations for exploring the role of ferroptosis in periodontitis. However, this study has several limitations. First, animal experiments are required to confirm the effects of *ACSL6* in periodontitis. Second, the analyzed dataset is relatively small, and other ferroptosis-related genes could

be involved in future studies on periodontitis. Third, the possible target proteins regulated by *ACSL6* are unclear; thus, the mechanism of *ACSL6* in periodontitis should be further investigated in future studies.

Conclusions

In this study, the mechanism underlying the involvement of the ferroptosis-related gene *ACSL6* in periodontitis was investigated. For the first time, we reported that *ACSL6* was highly expressed in periodontitis. Furthermore, *ACSL6*-mediated cell ferroptosis is mediated by *P. gingivalis*-LPS through the AMPK pathway. This study provides insight for exploring the mechanism of ferroptosis in periodontitis.

Availability of Data and Materials

All data generated or analyzed during this study are included in this published article.

Author Contributions

YX: conception and design of the study, critical revision of the manuscript for important intellectual content; YC and LC: acquisition of data; CZ, PL, OA, and YL: analysis and interpretation of data. YC, LC, CZ, PL, OA, YL, and YX contributed to the drafting and critical revision of the manuscript. All authors approved the version of the final manuscript. All authors have participated sufficiently in the work and agreed to be accountable for all aspects of the work.

Ethics Approval and Consent to Participate

The experiments were approved by the medical ethics committee of the Hospital of Stomatology, Guanghua School of Stomatology, Sun Yat-sen University (KQEC-2022-29-01), and informed consent was obtained from all participants by the Declaration of Helsinki.

Acknowledgment

Not applicable.

Funding

This work was supported by the National Natural Science Foundation of China [grant number 81771124].

Conflict of Interest

The authors declare no conflict of interest.

Supplementary Material

Supplementary material associated with this article can be found, in the online version, at https://doi.org/10.24976/Discov.Med.202537194.43.

References

[1] Zheng X, Chen J, Rao N, Yang C, Liu J, Zhang J, *et al*. The Effect of an Extract of Sappanwood, Protosappanin A and Protosappanin B on Osteogenesis in Periodontitis. Frontiers in Bioscience (Landmark Edition). 2023; 28: 172.

[2] Wang W, Zheng C, Yang J, Li B. Intersection between macrophages and periodontal pathogens in periodontitis. Journal of Leukocyte Biology. 2021; 110: 577–583.

[3] Hirtz C, O'Flynn R, Voisin PM, Deville de Périère D, Lehmann S, Guedes S, *et al*. The potential impact of salivary peptides in periodontitis. Critical Reviews in Clinical Laboratory Sciences. 2021; 58: 479–492.

[4] Xu J, Yin Y, Lin Y, Tian M, Liu T, Li X, *et al*. Long non-coding RNAs: Emerging roles in periodontitis. Journal of Periodontal Research. 2021; 56: 848–862.

[5] Zidar A, Kristl J, Kocbek P, Zupančič Š. Treatment challenges and delivery systems in immunomodulation and probiotic therapies for periodontitis. Expert Opinion on Drug Delivery. 2021; 18: 1229–1244.

[6] Mao H, Zhao Y, Li H, Lei L. Ferroptosis as an emerging target in inflammatory diseases. Progress in Biophysics and Molecular Biology. 2020; 155: 20–28.

[7] Zheng J, Conrad M. The Metabolic Underpinnings of Ferroptosis. Cell Metabolism. 2020; 32: 920–937.

[8] Yunchu Y, Miyanaga A, Seike M. Integrative Analysis of Ferroptosis-Related Genes in Small Cell Lung Cancer for the Identification of Biomarkers and Therapeutic Targets. Frontiers in Bioscience (Landmark Edition). 2023; 28: 125.

[9] Sun Y, Chen P, Zhai B, Zhang M, Xiang Y, Fang J, *et al*. The emerging role of ferroptosis in inflammation. Biomedicine & Pharmacotherapy. 2020; 127: 110108.

[10] Zhao Y, Li J, Guo W, Li H, Lei L. Periodontitis-level butyrate-induced ferroptosis in periodontal ligament fibroblasts by activation of ferritinophagy. Cell Death Discovery. 2020; 6: 119.

[11] Guzeldemir-Akcakanat E, Alkan B, Sunnetci-Akkoyunlu D, Gurel B, Balta VM, Kan B, *et al*. Molecular signatures of chronic periodontitis in gingiva: A genomic and proteomic analysis. Journal of Periodontology. 2019; 90: 663–673.

[12] Guzeldemir-Akcakanat E, Sunnetci-Akkoyunlu D, Orucguney B, Cine N, Kan B, Yılmaz EB, *et al*. Gene-Expression Profiles in Generalized Aggressive Periodontitis: A Gene Network-Based Microarray Analysis. Journal of Periodontology. 2016; 87: 58–65.

[13] Zou Y, Li C, Shu F, Tian Z, Xu W, Xu H, *et al*. lncRNA expression signatures in periodontitis revealed by microarray: the potential role of lncRNAs in periodontitis pathogenesis. Journal of Cellular Biochemistry. 2015; 116: 640–647.

[14] Jia L, Zhang Y, Ji Y, Li X, Xing Y, Wen Y, *et al*. Comparative analysis of lncRNA and mRNA expression profiles between periodontal ligament stem cells and gingival mesenchymal stem cells. Gene. 2019; 699: 155–164.

[15] Wan W, He C, Du C, Wang Y, Wu S, Wang T, *et al*. Effect of ILK on small-molecule metabolism of human periodontal ligament fibroblasts with mechanical stretching. Journal of Periodontal Research. 2020; 55: 229–237.

[16] Su W, Shi J, Zhao Y, Yan F, Lei L, Li H. Porphyromonas gingivalis triggers inflammatory responses in periodontal ligament cells by succinate-succinate dehydrogenase-HIF-1α axis.

Biochemical and Biophysical Research Communications. 2020; 522: 184–190.

[17] Sun K, Luo J, Jing X, Xiang W, Guo J, Yao X, *et al*. Hyperoside ameliorates the progression of osteoarthritis: An in vitro and in vivo study. Phytomedicine: International Journal of Phytotherapy and Phytopharmacology. 2021; 80: 153387.

[18] Teodoro BG, Sampaio IH, Bomfim LHM, Queiroz AL, Silveira LR, Souza AO, *et al*. Long-chain acyl-CoA synthetase 6 regulates lipid synthesis and mitochondrial oxidative capacity in human and rat skeletal muscle. The Journal of Physiology. 2017; 595: 677–693.

[19] Xie Z, Wang X, Luo X, Yan J, Zhang J, Sun R, *et al*. Activated AMPK mitigates diabetes-related cognitive dysfunction by inhibiting hippocampal ferroptosis. Biochemical Pharmacology. 2023; 207: 115374.

[20] Lee H, Zandkarimi F, Zhang Y, Meena JK, Kim J, Zhuang L, *et al*. Energy-stress-mediated AMPK activation inhibits ferroptosis. Nature Cell Biology. 2020; 22: 225–234.

[21] Plemmenos G, Evangeliou E, Polizogopoulos N, Chalazias A, Deligianni M, Piperi C. Central Regulatory Role of Cytokines in Periodontitis and Targeting Options. Current Medicinal Chemistry. 2021; 28: 3032–3058.

[22] Wang J, Zhou Y, Ren B, Zou L, He B, Li M. The Role of Neutrophil Extracellular Traps in Periodontitis. Frontiers in Cellular and Infection Microbiology. 2021; 11: 639144.

[23] Cekici A, Kantarci A, Hasturk H, Van Dyke TE. Inflammatory and immune pathways in the pathogenesis of periodontal disease. Periodontology 2000. 2014; 64: 57–80.

[24] Xu W, Zhou W, Wang H, Liang S. Roles of Porphyromonas gingivalis and its virulence factors in periodontitis. Advances in Protein Chemistry and Structural Biology. 2020; 120: 45–84.

[25] Shi J, Li J, Su W, Zhao S, Li H, Lei L. Loss of periodontal ligament fibroblasts by RIPK3-MLKL-mediated necroptosis in the progress of chronic periodontitis. Scientific Reports. 2019; 9: 2902.

[26] Yan B, Ai Y, Sun Q, Ma Y, Cao Y, Wang J, *et al*. Membrane Damage during Ferroptosis Is Caused by Oxidation of Phospholipids Catalyzed by the Oxidoreductases POR and CYB5R1. Molecular Cell. 2021; 81: 355–369.e10.

[27] Yuan H, Li X, Zhang X, Kang R, Tang D. Identification of ACSL4 as a biomarker and contributor of ferroptosis. Biochemical and Biophysical Research Communications. 2016; 478: 1338–1343.

[28] Angius A, Uva P, Pira G, Muroni MR, Sotgiu G, Saderi L, *et al*. Integrated Analysis of miRNA and mRNA Endorses a Twenty miRNAs Signature for Colorectal Carcinoma. International Journal of Molecular Sciences. 2019; 20: 4067.

[29] Quan J, Bode AM, Luo X. ACSL family: The regulatory mechanisms and therapeutic implications in cancer. European Journal of Pharmacology. 2021; 909: 174397.

[30] Chen WC, Wang CY, Hung YH, Weng TY, Yen MC, Lai MD. Systematic Analysis of Gene Expression Alterations and Clinical Outcomes for Long-Chain Acyl-Coenzyme A Synthetase Family in Cancer. PLoS ONE. 2016; 11: e0155660.

[31] Su RJ, Jonas BA, Welborn J, Gregg JP, Chen M. Chronic eosinophilic leukemia, NOS with t(5;12)(q31;p13)/ETV6-ACSL6 gene fusion: a novel variant of myeloid proliferative neoplasm with eosinophilia. Human Pathology (New York). 2016; 5: 6–9.

[32] Liu T, Yuan Z, Wang H, Wang J, Xue L. Peroxisome-related genes in hepatocellular carcinoma correlated with tumor metabolism and overall survival. Clinics and Research in Hepatology and Gastroenterology. 2022; 46: 101835.

[33] Liang Y, Sun HX, Ma B, Meng QK. Identification of a Genomic Instability-Related Long Noncoding RNA Prognostic Model in Colorectal Cancer Based on Bioinformatic Analysis. Disease Markers. 2022; 2022: 4556585.

[34] Carling D. AMPK signalling in health and disease. Current Opinion in Cell Biology. 2017; 45: 31–37.

[35] Jung TW, Park HS, Choi GH, Kim D, Lee T. β-aminoisobutyric acid attenuates LPS-induced inflammation and insulin resistance in adipocytes through AMPK-mediated pathway. Journal of Biomedical Science. 2018; 25: 27.

[36] Tan C, Gu J, Li T, Chen H, Liu K, Liu M, *et al*. Inhibition of aerobic glycolysis alleviates sepsis induced acute kidney injury by promoting lactate/Sirtuin 3/AMPK regulated autophagy. International Journal of Molecular Medicine. 2021; 47: 19.

[37] Jung TW, Pyun DH, Kim TJ, Lee HJ, Park ES, Abd El-Aty AM, *et al*. Meteorin-like protein (METRNL)/IL-41 improves LPS-induced inflammatory responses via AMPK or PPARδ-mediated signaling pathways. Advances in Medical Sciences. 2021; 66: 155–161.